International Journal of Engineering Materials and Manufacture (2026) 11(1) 6-19
https://doi.org/10.26776/ijemm.11.01.2026.02

Experimental and Finite Element Analysis of Heat Conduction of Brass, Copper and Aluminium

Azhin Abdallah Abdalrahman, Hawre F. Amin and Pshtiwan M. Karim

Received: 11 November 2025
Accepted: 13 January 2026
Published: 30 January 2026
Publisher: Deer Hill Publications

ABSTRACT
Thermal conductivity is the transmission of internal energy through electron movement or lattice vibrations within a substance from an area with warmer temperatures to one with lower temperatures between two adjacent materials. Kinetic activity escalates with temperature, resulting in accelerated molecular motion. This study examined the linear heat conductivity of three distinct samples: brass, copper, and aluminium. This was achieved by attaching the thermocouples and electric heater to the sockets on the Heat Transfer Experiments Base Unit (TD1002A), which also serves as the heat sink's cold-water input and drain. The experimental base unit was utilized to achieve seven different temperatures; simultaneously, seven different temperatures were studied by the finite element analysis method (Ansys Workbench). Analysis of the gathered data revealed that, the temperature decreases progressively along the measurement points for all materials. Brass shows a reduction from 58 °C to 27 °C, copper from 55 °C to 28 °C, and aluminium from 58 °C to 29 °C. Among the tested materials, brass exhibits the largest overall temperature drop, while copper demonstrates the most uniform thermal decline, indicating material-dependent heat transfer behaviour. similarly, the results of finite element showed nearly the same values as the experimental results.
Keywords: Thermal conductivity, Finite element analysis, Brass, Copper, Aluminium.

1 INTRODUCTION
One branch of engineering science is heat transfer that examines the movement of energy due to temperature differentials. When two cold and hot materials come into touch, kinetic energy is transmitted through the contact edge. Energy is moved from the molecules in the hotter material to the molecules in the cooler material. The hotter material loses heat while the cooler material gains heat (Yener and Kakac,2018; Kurian et al., 2016). Thermal conduction is a capacity of substance to transfer heat and is a crucial metric for assessing its heat conduction properties. Thermal conductivity value signifies the value at which heat transfers from a specific substance. The velocity of a molecule correlates directly with its energy transfer efficiency (Tritt,2005; Han et al.,2022). The heat transfer through a cylindrical rod under a one-dimension temperature with a tiny cross-sectional area, is directly correlated with the cross-sectional area, The difference in temperature between both sources, and the material's thermal conductivity. This relationship is ruled by heat conduction Fourier's rule (William et al., 2009; Liu et al., 2017; Kosbe et al., 2019).

Boltzmann transport equation indicates that the temperature distribution varies with both time and spatial location. After a period, heat transfer reaches a steady state, resulting in a temperature difference between two points for each unit dimension of the rod. This variance represents the temperature gradient distribution equation as a position function. The material thermal conductivity is directly proportional to its capability to conduction heat, with a higher thermal conductivity coefficient indicating superior heat transfer capabilities (Padrah et al., 2019). Materials that are used as conductors are excellent at carrying electricity. Following this concept, the thermal conductions and electrical of comparable materials are measured and studied using the Lorenz number that is derived (Wang et al., 2018; Devaramani et al., 2025). Accurate direct temperature measurement is essential for reducing heat loss to and from the surrounding environment. Because the system is susceptible to environmental impacts, the computation results need to be adjusted (Holman et al., 2010). For both pure and mixed materials, the thermal conductivity value has been calculated using different methods. The steady-state approach, transient laser flash diffusivity, the (hot)-wire technique, and the temporary plane basis method are the most commonly employed for thermal characterization of bulk materials (Miranda et al., 2016). The 3ω methods, which combine frequency-domain and time-domain analysis, are commonly used for measuring of thin films, as is the temporary fluctuance technique (Zhao et al., 2018; Jalali et al., 2021).

Azhin A. A., Hawre F. A.✉ and Pshtiwan M. K.
Department of Mechanic (CAD-CAM), Sulaimani Technical Institute
Sulaimani Polytechnic University, Sulaimani, Iraq
E-mail: azhin.a.abdulrahman@spu.edu.iq

Reference: Azhin et al. (2026). Experimental and Finite Element Analysis of Heat Conduction of Brass, Copper and Aluminium. *International Journal of Engineering Materials and Manufacture*, 11(1), 6-19.

Thermal conductivity is a relative property that changes with respect to humidity, material density, and surrounding temperature (Rasaq et al., 2018). (Two) calorimeters, one full of cold water and the other with hot water, will be used to measure the thermal conductivity of a substance (Blackwell et al., 2000). The Fourier equation measures the correlation within the one-dimensional x-direction heat transfer value and the conducting medium's characteristics and temperature gradient (Abdullah et al., 2019; Zain-ul-abdein et al., 2015). Thermal contact conductance (TCC) was investigated in relation to asperity height and the number of discrete contact points by (Ajul et al., 2021). Effect of laser beam variation on melt flow and temperature field during laser welding brass and 308 stainless steel {S.S. 308} was investigated both empirically and numerically by (Zhang et al., 2025).

Two approaches for generating rough surfaces with varying roughness values have been created by random number generation utilising universal finite element analysis in ANSYS (Rana and Kumar, 2019). An examination of heat transmission during the of Al12%Si (LM 13) alloy solidification is conducted by gathering the history of the solidifying temperature casting (Hemanth 2014). The coupled Eulerian Lagrangian approach in Abaqus software has been employed to conduct Al 1050 micro frictional stirring welding to natural copper using finite element analysis (Mahdianikhotbesara et al., 2022). Conversel, (Talaghat et al., 2017) proposed research on the assessment of heat transfer variable, specifically the thermal diffusivity and factor, employing experimental numbers and analytical resolutions for standard geometric shape, including infinite slabs, infinite cylinders, and spheres.

Furthermore, (Xu et al., 2019) explained the thermal efficacy and hydrodynamic of blocks of brass wire mesh in a vertical canal. The brass wire meshes that are available are positioned adjacently to function as a puros block. (Khoshaim et al., 2024) investigated the freezing process inside a tank featuring a rounded cool surface, using a novel application of fins. The incorporation of paddles and the deliberate integration of nanomaterials significantly improve hardening efficiency, through prospective uses in cryopreservation and thermal energy storage. To dynamically influence macroscopical thermal phenomenon in artificial systems, which allows individuals to alter heat phenomena at will, (Yang et al., 2021) employed thermal metamaterials to regulate macroscopic heat transmission. A solution for reducing the restoring relaxation time based on experimental temperature field values has been developed by (Formalev et al., 2018).

Conversely, (Abbasi et al., 2017) explained research for analysing the procedure for injecting (cold) water into a completely piercing well containing evenly space out horizontal breakages within a breakages geothermal tank. (Li et al., 2021) presented a cohesive framework for heat transfer control, suggesting that related research can be viewed as complementary approaches to manipulating physical parameters and achieving novel phenomena in heat transfer through artificial structures, including thermal conductivity in conduction, thermal emissivity in radiation, and properties associated with multiphysical effects. Furthermore (Lin et al., 2025) created a sample of gas-saturated hydrate in sand sediment and thermal Encouragement. it through an essential injection well prompted hydrate separation. An enhanced organizational design of a (water)cooled beam in a warming furnace of the walking beam type, based on the heat transfer model that combines conduction and radiation provided by (Xu et al., 2025). The impact of thermal conductivity in the cylinder wall on high-pressure liquid hydrogen pumps' in-cylinder heat transfer was presented by (Qiu et al., 2025). Conversely, (Chen, 2025) Proposed Heat and moisture transport by conduction and convection in the elastic's open-width pre-drying textiles.

However, previous studies have predominantly employed either experimental methods or finite element analyses independently to investigate the thermal conductivity behaviour of various metals. Limited research has focused on a direct comparison between experimental results obtained from (Heat transfer experimental base unit (TD1002)) and ANSYS finite element simulations to accurately predict temperature distribution and thermal behaviour of the three device rods.

2 METHODOLOGY

In the present study, the thermal conductivity value will be evaluated by connecting the thermocouples and electric heater to the outlets on the base unit for the heat transfer experiment (TD1002A). Additionally, this unit provides the heat sink's cold-water feed and outflow. The produce of the path's length and the amount of temperature variation and the amount of heat of energy delivered per time unit is known as the gradient of temperature. Fourier equation provides a mathematical representation of the link among the x-direction one-dimensional heat transfer amount, the gradient of temperature and parameters of the medium that conducts (Holman et al., 2010). As stated, the rate at which thermal energy is transferred across a unit length of substance with a unit cross-sectional area is known as thermal conductivity. Consequently, for the solid bar:

$$\dot{Q} = kA\frac{T_1 - T_2}{L} \quad (1)$$

In order to find thermal conductivity of material, the equation should be rearranged to provide:

$$k = \dot{Q} \times \frac{L}{A(T_1 - T_2)} \quad (2)$$

Furthermore, the equation can be written in terms of thermal resistance. This rate is valuable for engineers in which they can select proper materials when it is needed to stop heat transfer, or to isolate a structure or a machine component.

$$Thermal\ Resistance\ (R) = \frac{L}{kA} \quad [k/w] \quad (3)$$

The electrical power into the heater is the product of the voltage and current supplied to it, so:

Electrical power (W) = voltage (V) across the heater × current (I) passing through the heater

$$W = V \times I \tag{4}$$

The unit (watt) of electrical power is also a measurement of rate of energy transfer (one joule per second), so:

$$W = \dot{Q} \tag{5}$$

This indicates that the heater's internal energy (heat) transmission rate is equivalent to the electrical energy provided to it.

2.1 Linear Heat Conduction Experiment

This research involves a solid brass rod with a round cross section, constructed in both segments featuring an adjustable central piece. It is affixed to a foundation plate featuring a transparent schematic of the test configuration. The offered transposable middle portions are composed of several metals, including brass, copper, and aluminium. Each central part contains three thermocouples to facilitate the estimation of the specimens' thermal conduction. The thermocouples and electric heater are connected to the heat transfer experiments base unit's sockets, which similarly provides the cold water heat sink feed and drainage, as illustrated in Fig. 1.

Initially, configure and connect the experiment (TD 1002A) as depicted in Fig. 1. to facilitate the experimentation. Subsequently, Put the middle brass section on utilizing heat transfer paste. Additionally, employ a precise thermometer to determine the temperature of the surrounding air in the area as a guide, as showed in Fig. 2.

Then, the water output valve should be opened to let water flow, turn on the heater and adjust the power to 30W. Furthermore, allow the temperatures to steady before recording T1 to T7. Deactivate the water supply and heater. Reiterate the preceding procedures by installing copper and aluminium intermediary segments. Examine a cylindrical bar depicted as shown in Fig 3, where the temperature at T1 exceeds that at T7. Thermal energy transfers from the area at temperature T1 to the area at temperature T7. Table 1. illustrates the required information the bars used in this experiment. According to the data in Table 1, thermal conductivity for the three circular rods (brass, copper and aluminium) can be found and compare with the Ansys thermal conductivity.

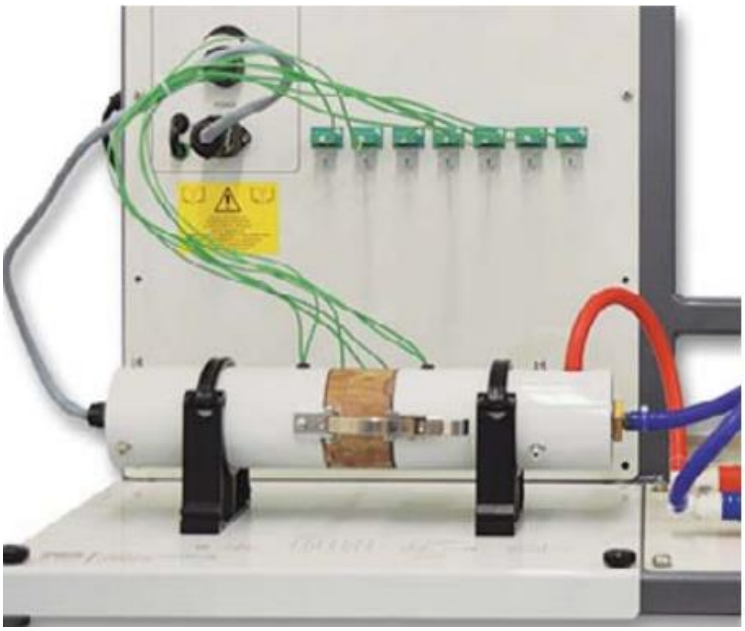

Figure 1: Heat transfer experimental base unit (TD1002).

Table 1: The data required for determine the experimental thermal conductivity

Circular bar material	Brass, copper and aluminium
Bars diameter(D)	30 mm
Bars length(L)	120mm
Thermocouples	T1, T2 T3 T4 T5 T6 T7 equally spaced radius
Heater power ($\dot{Q}$)	30 watts

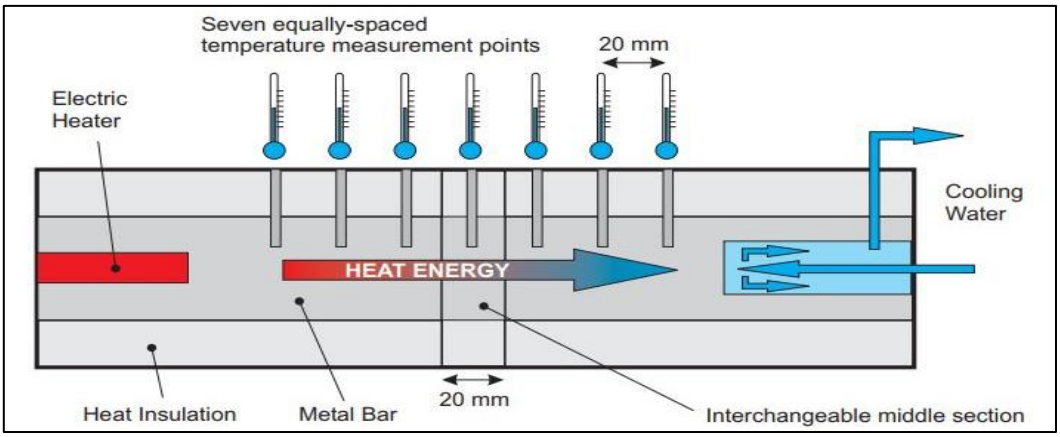

Figure 2: Linear heat conduction

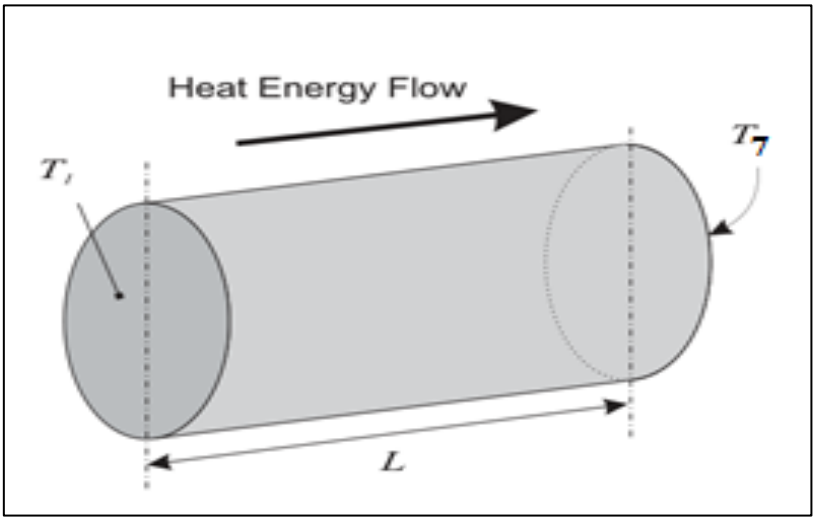

Figure 3: Circular bar cross section of samples

2.2 Finite Element Analyses

This study analysed the steady-state thermal properties of three rods: brass, copper, and aluminium. A finite element analysis was conducted utilizing the ANSYS software package (version 15.0). ANSYS Workbench is a prevalent program for engineering problem-solving. Common operations executed within ANSYS Workbench encompass importing models from many CAD systems, managing engineering data, utilizing Design Modeller, generating models, configuring solver parameters, and analysing results. The Design Modeller is mostly utilized for geometry creation, while the model is employed for mesh production and boundary condition establishment. The stages necessary for completing finite element modelling can be summarized as follows:

The steady state thermal was selected in the first step for the three rods Brass, Copper and aluminium. as shown in Fig. 4. In the second step enter isotropic thermal conductivity in the Engineering data module as shown in Table.2. And create all three geometries separately in three steady thermal state, see Fig. 5.

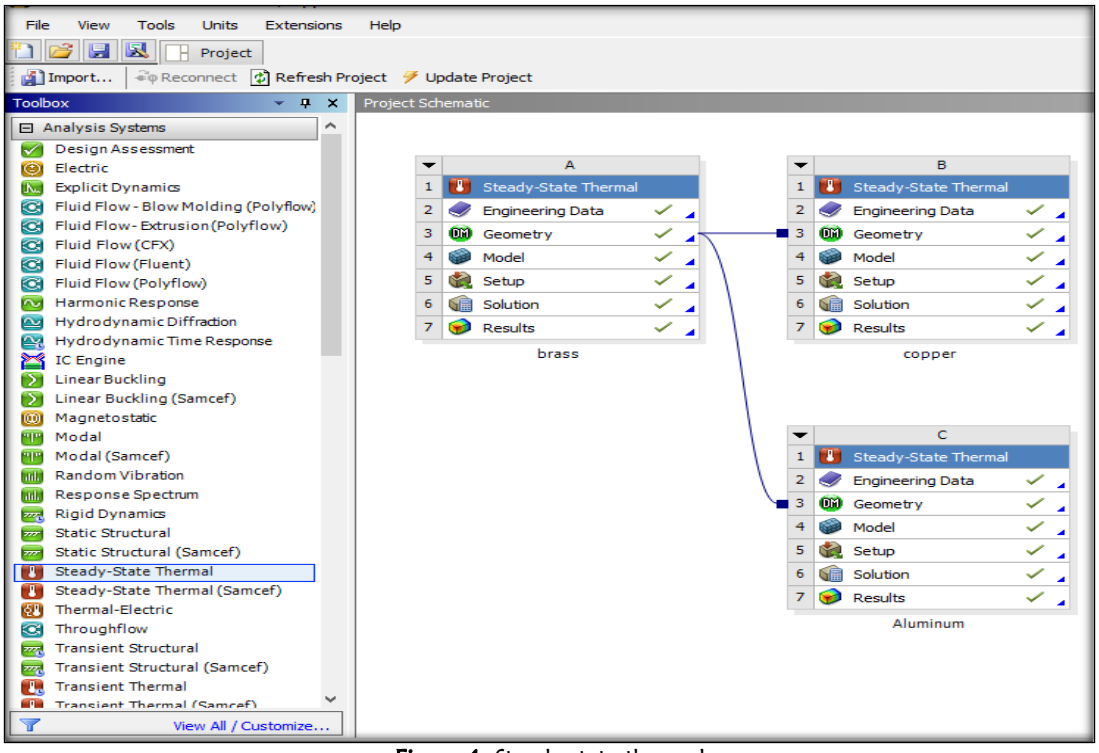

Figure 4: Steady state thermal

Table 2: Engineering data module

Material	Brass	Copper	aluminium
Isotropic thermal conductivity	$111 w.m^{-1}c^{-1}$	$400 w.m^{-1}c^{-1}$	$237.5 w.m^{-1}c^{-1}$

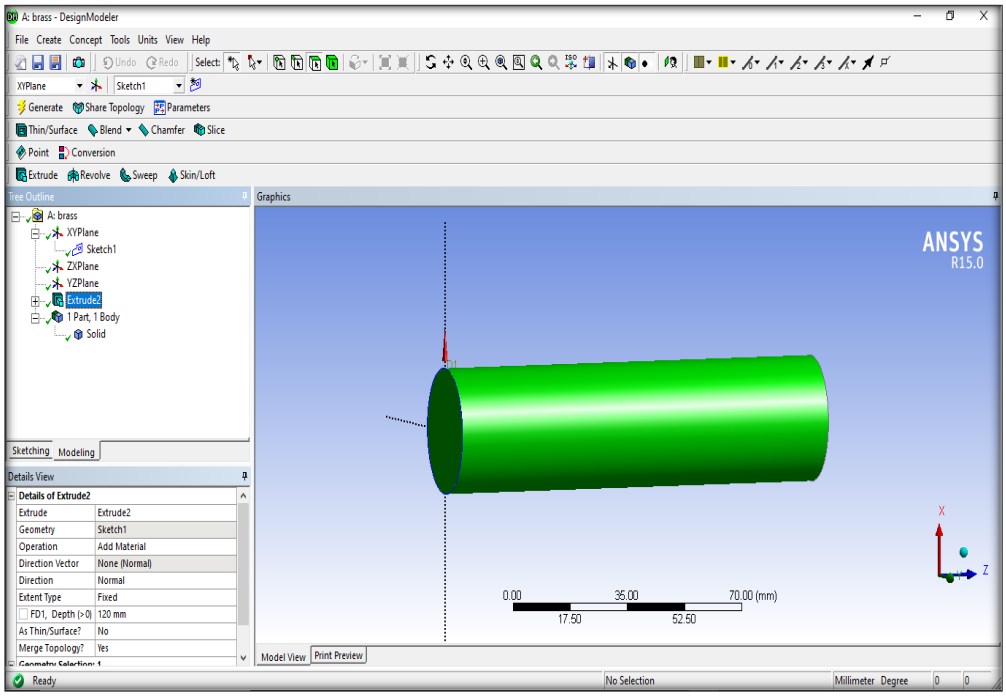

Figure 5: Geometry of the rods

After creating the geometries, we built a mesh for the three geometry models as shown in the Fig.6 . (a), (b), (c).

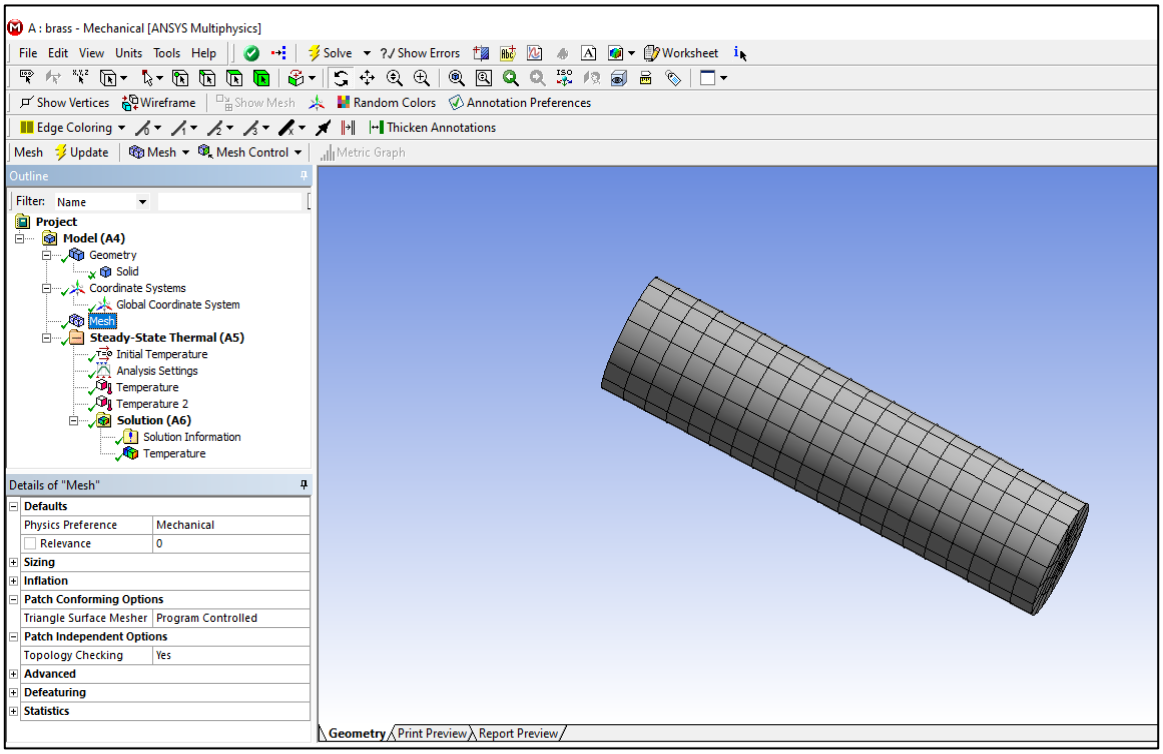

(a) Meshing of the brass rod

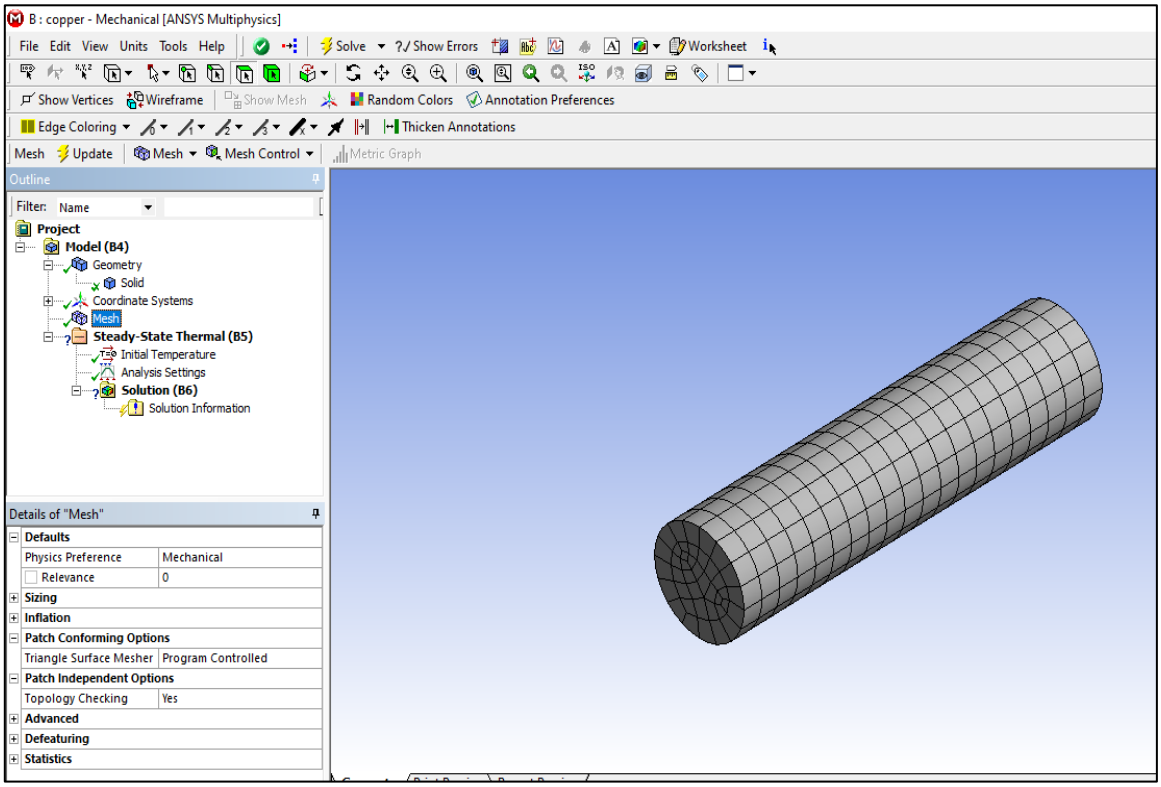

(b) Meshing of the copper rod

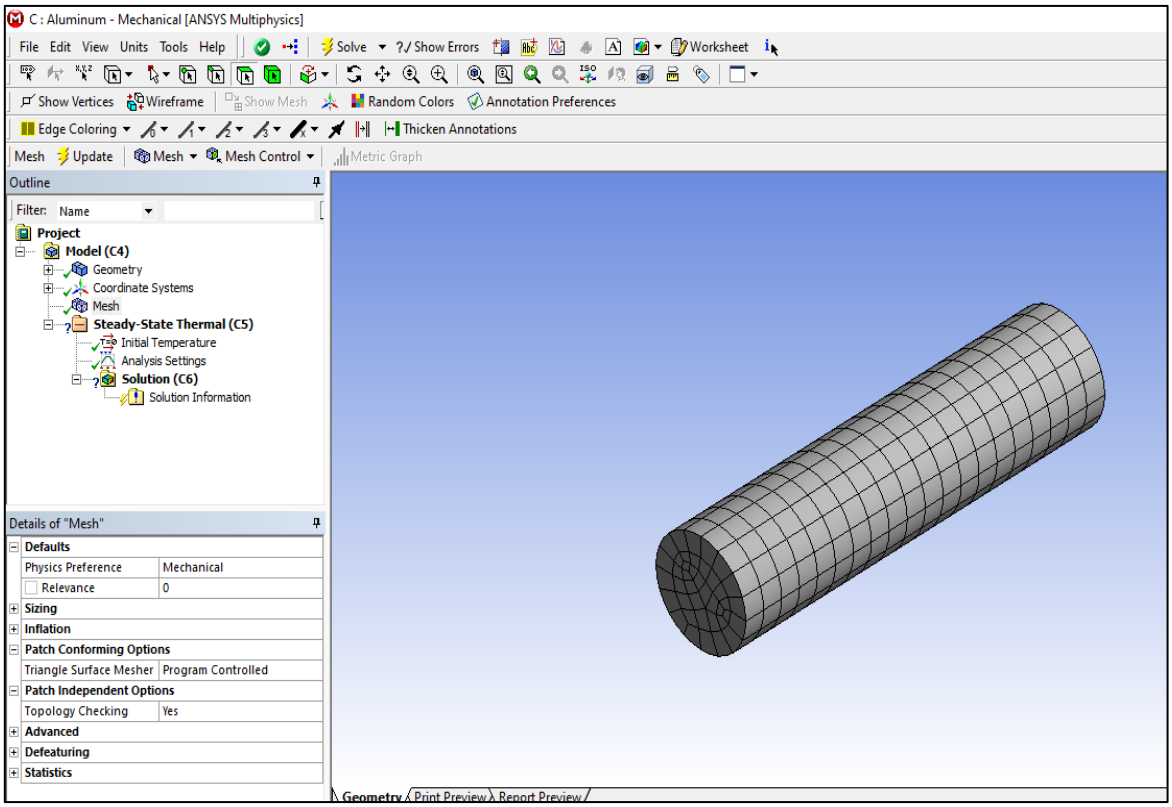

(c) Meshing of the Aluminum rod

Figure 6: Generating a mesh for the (brass, copper and aluminium) rod.

The fourth step is choosing the material and inserting the temperatures on the rods, see Fig. 7(a), (b), (c).

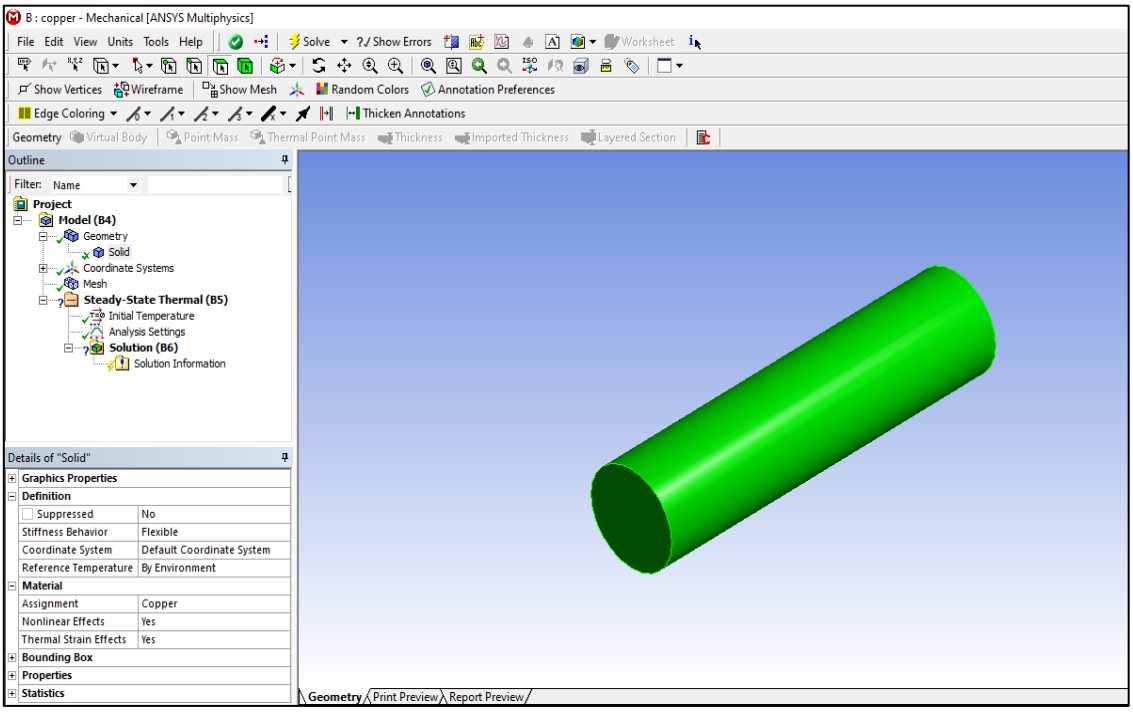

(a) Insert temperature for the copper rod

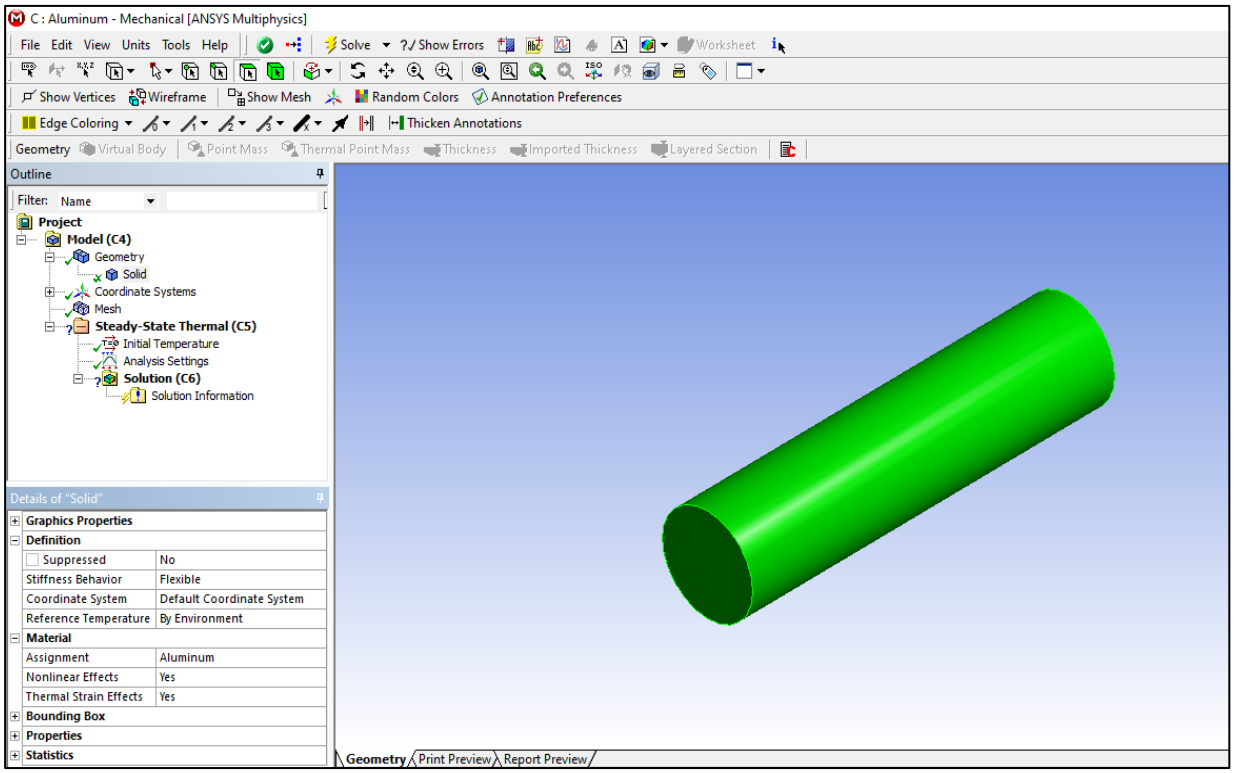

(b) Insert temperature for the aluminium rod

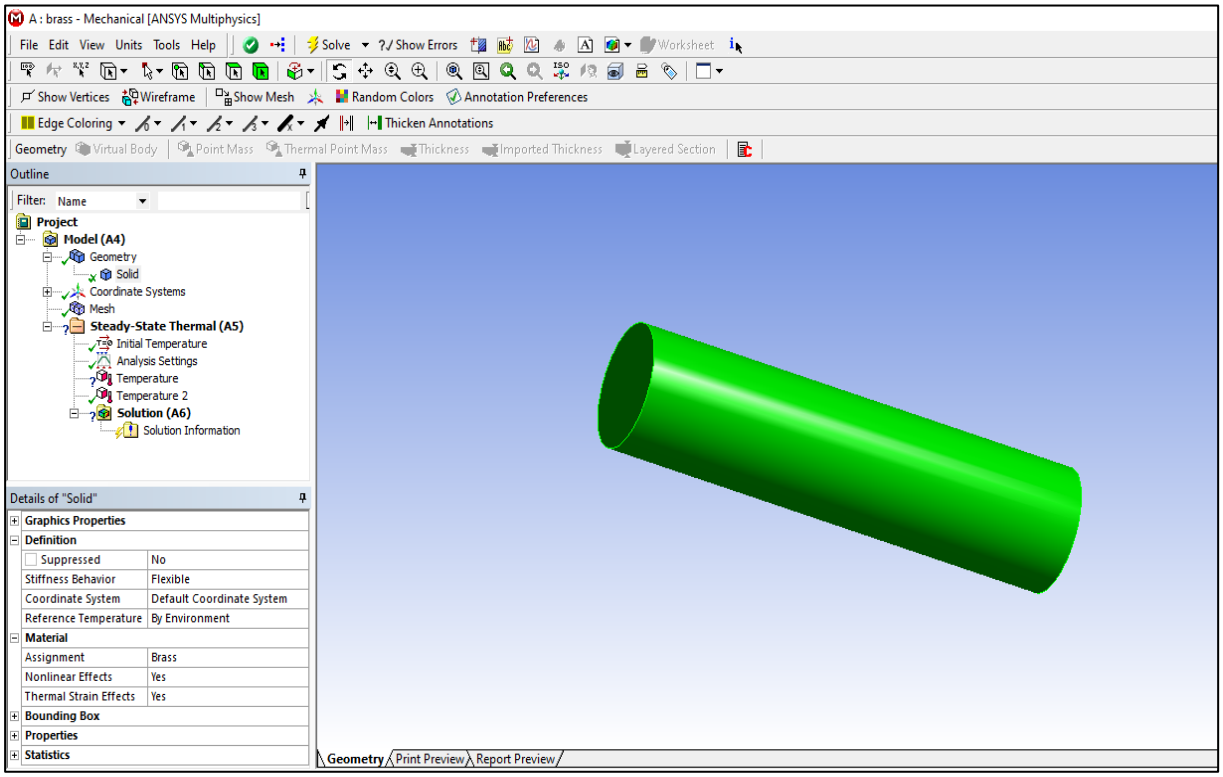

(c) Insert temperature for the brass rod

Figure 7: Choosing the materials and inserting temperatures for the rods.

3 RESULTS AND DISCUSSIONS

In this paper to identify the materials ability to conduct heat by using the heat transfer experimental base unit, seven different temperatures were found and based on those data's we found thermal conductivity, see table 3. For more explanation of the temperature gradient of the three rods, we created three graphs between the distance and temperatures, see Fig. 8, 9, and 10.

Table 3: the achieved temperatures from the heat transfer experiments base unit and thermal conductivity.

Material	T1$\mathbf{c}^{\circ}$	T2 $\mathbf{c}^{\circ}$	T3 $\mathbf{c}^{\circ}$	T4 $\mathbf{c}^{\circ}$	T5 $\mathbf{c}^{\circ}$	T6 $\mathbf{c}^{\circ}$	T7 $\mathbf{c}^{\circ}$	Thermal conductivity (K) (Experimental) $\mathbf{w.m^{-1}c^{-1}}$
Brass	58	54	49	45	34	31	27	164.3
Copper	55	51	47	43	36	32	28	189.4
Aluminium	58	53	48	43	38	33	29	176.4

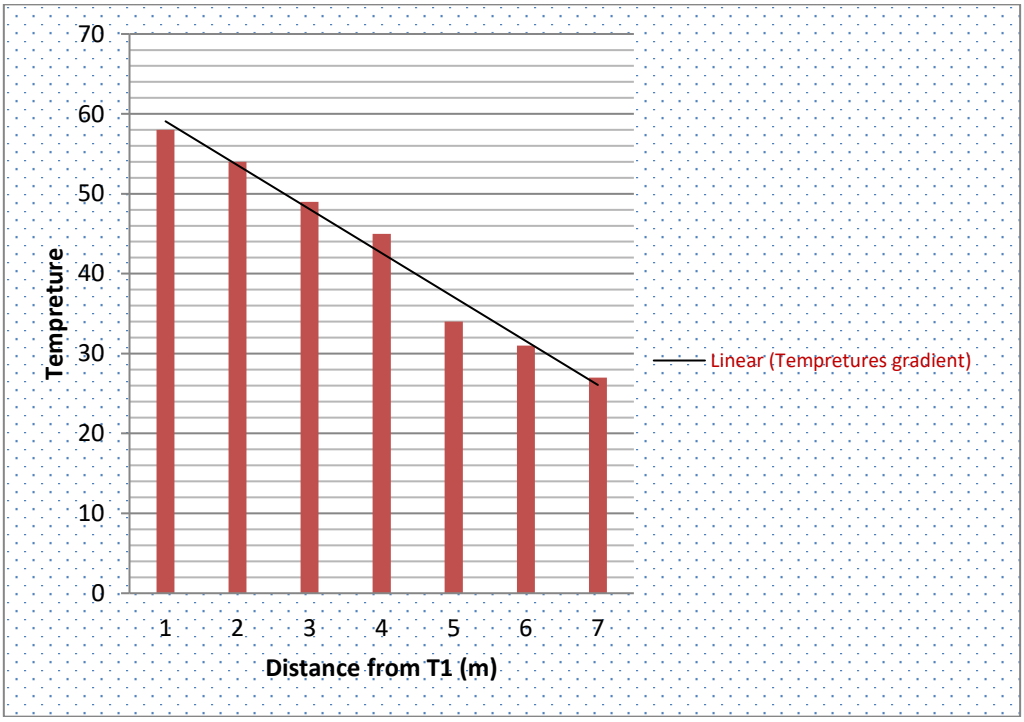

Figure 8: The temperature gradient of Brass rod

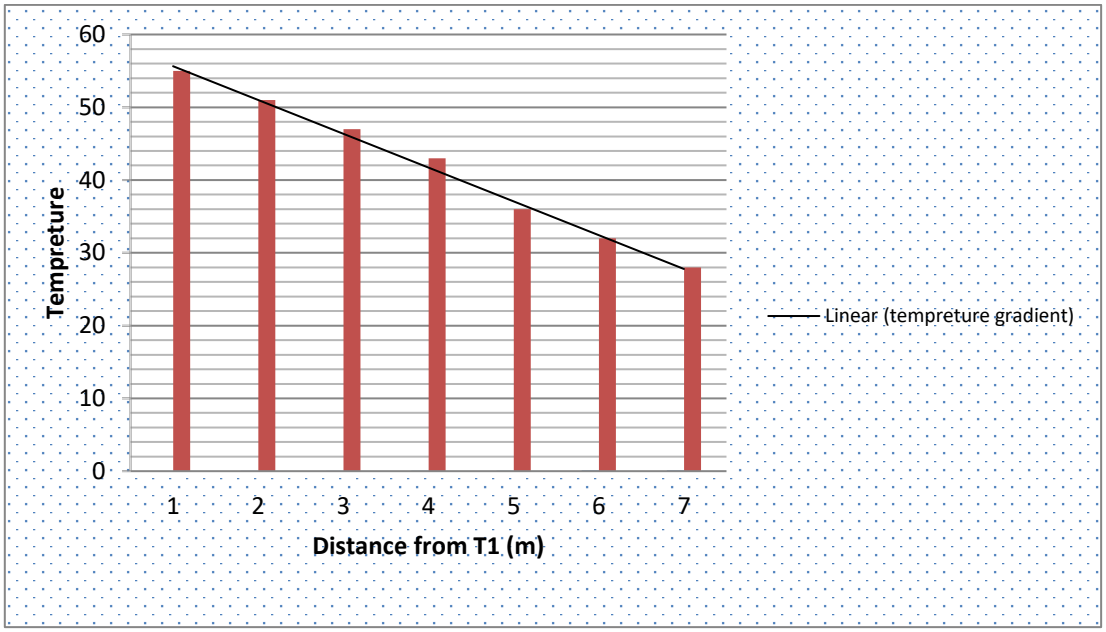

Figure 9: The temperature gradient of copper rod

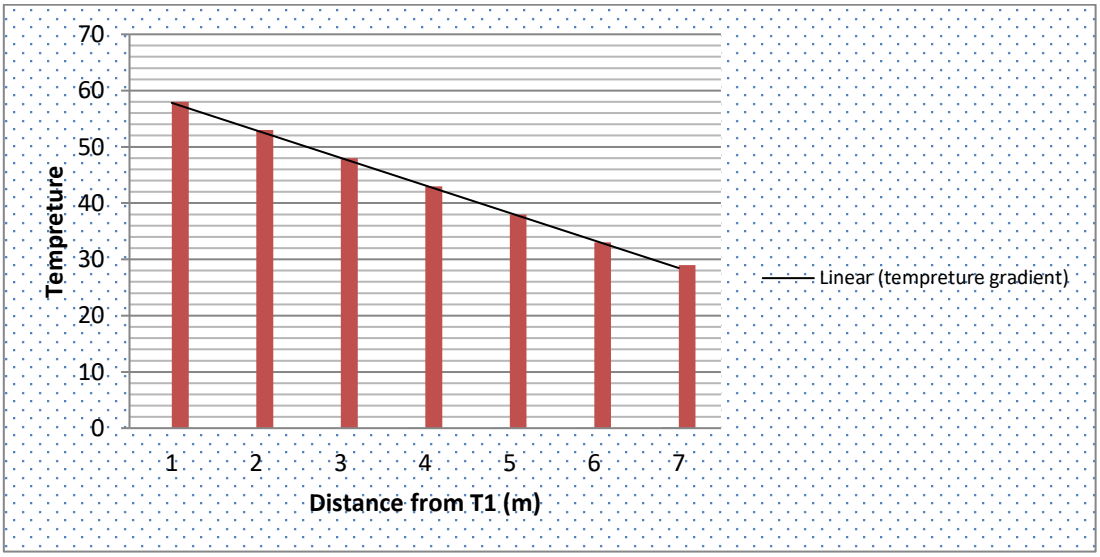

Figure 10: The temperature gradient of aluminium rod

According to the curves gradient it can be seen that by remote thermocouples on the rods from the heat source, the temperature decreases have low temperatures as compared to near thermocouples, so T1 has greater temperature value than T7 in all the three graphs, because the first thermocouple has the nearest location from the electric heater. It is also in the finite element analysis ANSYS package (release 15.0) thermal steady state was performed for the three different rods. The results of the analysis can be seen in the Fig. 11.(a),(b),(c).

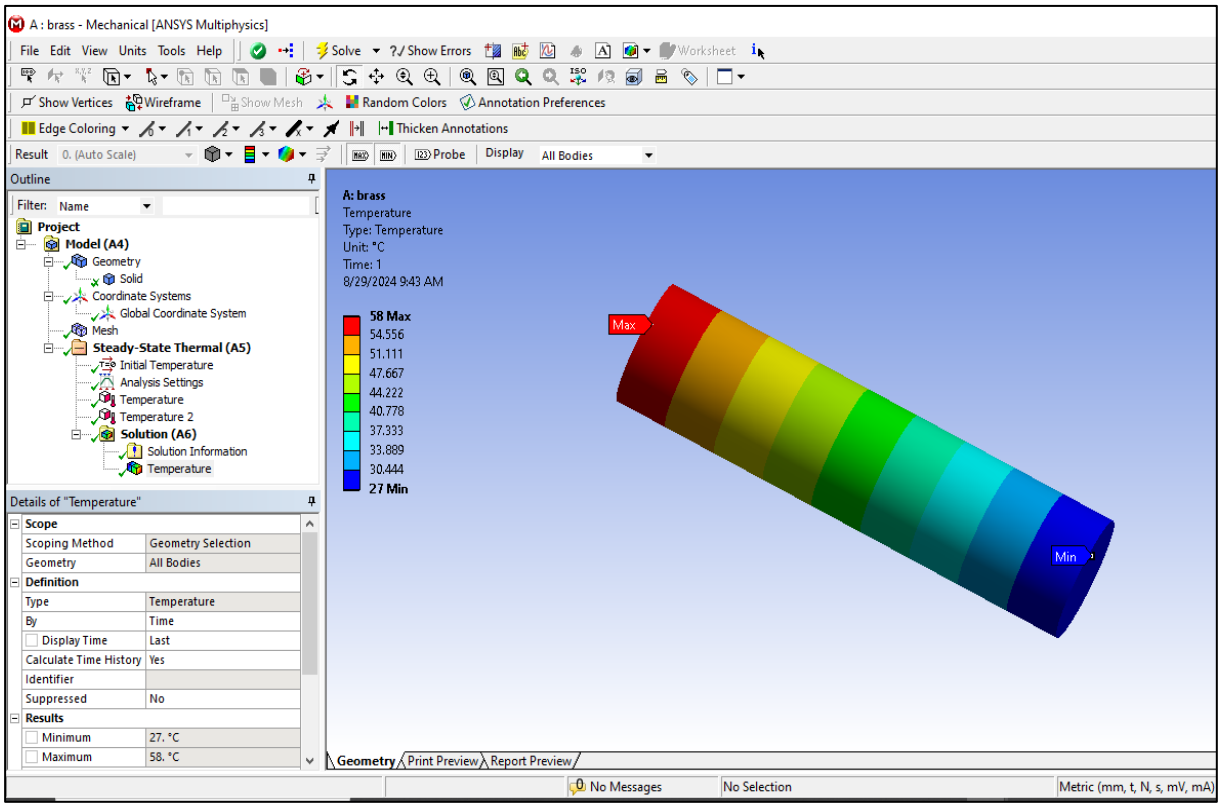

(a) Solution for brass rod

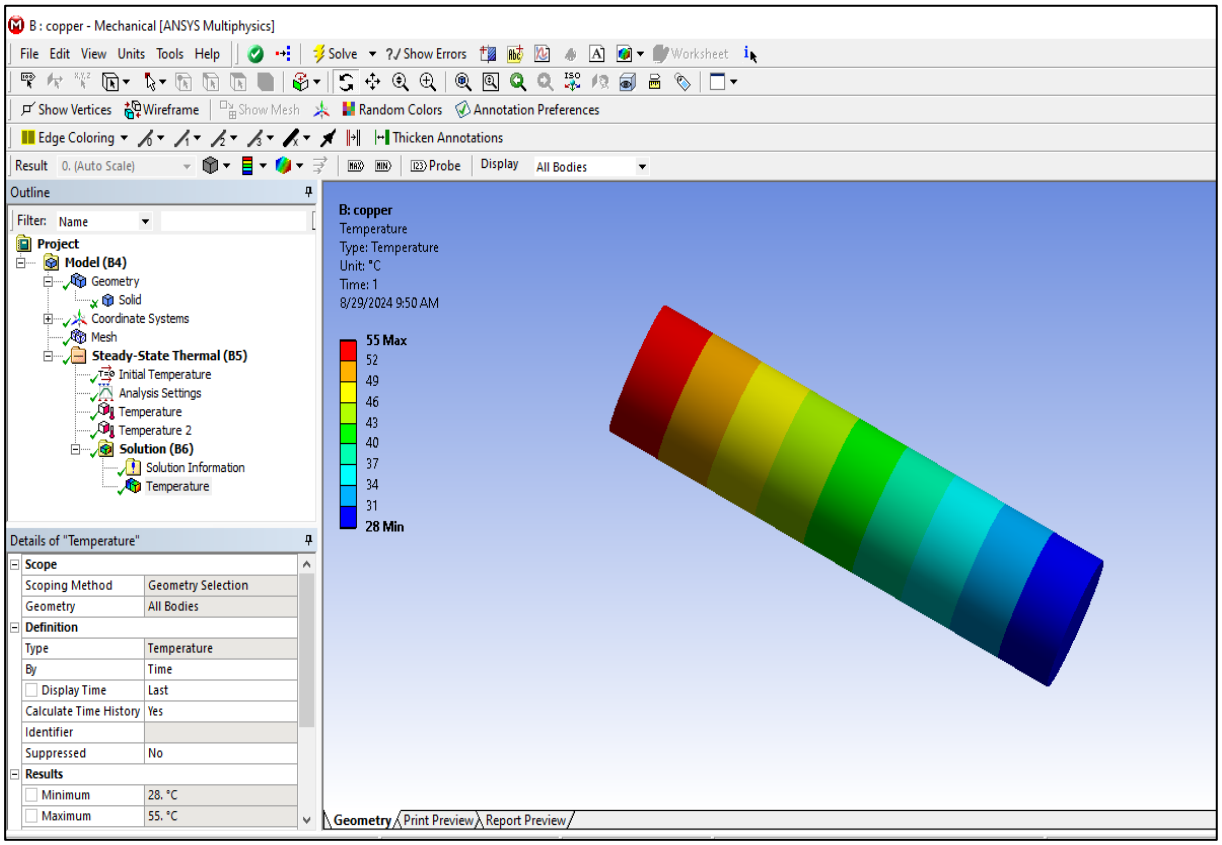

(b) Solution for copper rod

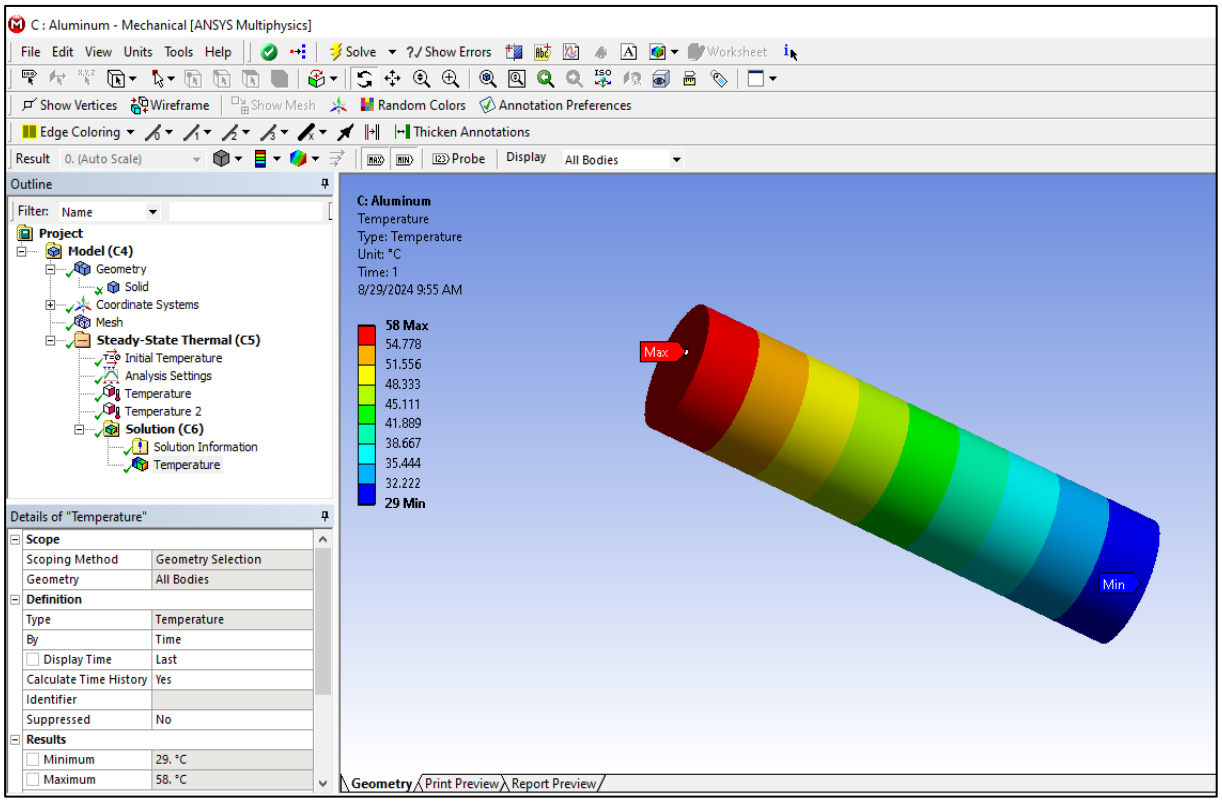

(c) Solution for aluminium rod

Figure 11: Solution of the (brass, copper and aluminium) rods (a), (b), (c)

The achieved temperatures from the finite element method can be seen in table 4.

Table 4: The achieved temperatures from the finite element method

Material	T1	T2	T3	T4	T5	T6	T7	T8	T9	T10
Brass	58	54.4	51.1	47.6	44.2	40.7	37.3	33.8	30.4	27
Copper	55	52	49	46	43	40	37	34	31	28
Aluminium	58	54.7	51.5	48.3	45.11	41.88	34.6	35.4	32.2	29

From the table above it can be shown (ten) different temperatures for the three different materials, which all of those temperatures were received from thermal steady state analyses. Brass and aluminium have the highest temperature rate as compared to copper and the lowest temperatures value was recorded by brass material.

4 CONCLUSIONS

1. In this paper by using the heat transfer experimental base unit seven different temperatures were found.
2. According to the experimental data, T1 has greater temperature value than T7 in all the three graphs, because the first thermocouple has the nearest location from the electric heater.
3. It is also observed from the research that copper has the maximum value of thermal conductivity as compared to brass and aluminium.
4. In the finite element analysis ANSYS package (release 15.0) thermal steady state was performed for the three different rods.
5. 5.(T1) According to the finite element analysis also has the greatest value for aluminium, copper and brass as compared to another temperatures.
6. Comparing the result between the samples, it can be seen that temperature fall gradually from T1 to T7 in both experimental and finite element analysis.

REFERENCE

1. Abbasi, M., Khazali, N., & Sharifi, M. (2017). Analytical model for convection–conduction heat transfer during water injection in fractured geothermal reservoirs with variable rock matrix block size. *Geothermics*, *69*, 1–14. https://doi.org/10.1016/j.geothermics.2017.04.002

2. Abdullah, N. S., Yusoff, H., Zaba, H. S., Ghafar, H., Farhan, A., Budin, S., & Suhaimi, S. (2019). An experimental study on thermal conductivity of T2 copper with different surface roughness. *Journal of Physics: Conference Series, 1349*, 012039. https://doi.org/10.1088/1742-6596/1349/1/012039
3. Ajul, E., Kishor, E., & Chanda, S. (2021). Prediction of thermal contact conductance in conforming rough metal contacts through regeneration of surface profile. In *Proceedings of the 26th National and 4th International ISHMT–ASTFE Heat and Mass Transfer Conference*. Begell House Inc. http://dx.doi.org/10.1615/IHMTC-2021.2620
4. Blackwell, B. F., et al. (2000). *Determination of thermal conductivity of 304 stainless steel using parameter estimation techniques* (Report No. SAND2000-1563C). Sandia National Laboratories.
5. Chen, H., Shu, W., Li, G., Lian, S., Mao, Z., & Zhou, D. (2025). Conduction–convection coupled heat and moisture transfer in the open-width pre-drying for elastic fabrics. *International Journal of Thermal Sciences, 215*, 109963. https://doi.org/10.1016/j.ijthermalsci.2025.109963
6. Devaramani, K. S., Sreenivasa, T. N., Dadapeer, B., et al. (2025). Finite element and experimental analysis of CuZn37 brass alloy's mechanical and formability properties at different annealing temperatures. *Journal of The Institution of Engineers (India): Series D*. https://doi.org/10.1007/s40033-025-00863-4
7. Formalev, V. F., Kolesnik, S. A., & Kuznetsova, E. L. (2018). On the wave heat transfer at times comparable with the relaxation time upon intensive convective–conductive heating. *High Temperature, 56*, 393–397. https://doi.org/10.1134/S0018151X18030069
8. Han, J.-C., & Wright, L. (2022). *Analytical heat transfer* (2nd ed.). CRC Press. https://doi.org/10.1201/9781003164487
9. Hemanth, J. (2014). Heat transfer analysis during external chilling of composite material castings through experimental and finite element modelling. *Modeling and Numerical Simulation of Material Science, 4*(1), 1–7. https://doi.org/10.4236/mnsms.2014.41001
10. Holman, J. P. (2010). *Heat transfer* (10th ed.). McGraw-Hill.
11. Yener, Y., & Kakaç, S. (2018). *Heat conduction*. CRC Press. https://doi.org/10.1201/9780203752166
12. Jalali, A., Hashemi, R., Rajabi, M., & Tayebi, P. (2021). Finite element simulations and experimental verifications for forming limit curve determination of two-layer aluminum/brass sheets. *Journal of Materials: Design and Applications, 236*(2), 361–373. https://doi.org/10.1177/14644207211045212
13. Khoshaim, A., Basem, A., Hussein, A. Z., Al-Bonsrulah, N. H., Abu-Hamdeh, N. H., Mohamed, S. M. Y., & Milyani, A. H. (2024). Incorporating numerical method for analyzing conduction heat transfer during solidification loading nanoparticles. *Case Studies in Thermal Engineering, 64*, 105383. https://doi.org/10.1016/j.csite.2024.105383
14. Kosbe, P., & Patil, P. A. (2019). Effective thermal conductivity of polymer composites: A review of analytical methods. *International Journal of Ambient Energy, 42*(8), 961–972. https://doi.org/10.1080/01430750.2018.1557544
15. Kurian, R., Balaji, C., & Venkateshan, S. P. (2016). Experimental investigation of convective heat transfer in a vertical channel with brass wire mesh blocks. *International Journal of Thermal Sciences, 99*, 170–179. https://doi.org/10.1016/j.ijthermalsci.2015.08.002
16. Li, Y., Li, W., Han, T., Zheng, X., Li, J., Li, B., & Qiu, C. W. (2021). Transforming heat transfer with thermal metamaterials and devices. *Nature Reviews Materials, 6*(6), 488–507. https://doi.org/10.1038/s41578-021-00283-2
17. Lin, D., Liu, J., Lu, J., Ma, K., Zhang, Q., Li, D., Xia, Z., Li, X., & Liang, D. (2025). Convection–conduction heat transfer and seepage in hydrate-bearing sandy sediments under hot fluid injection. *Energy, 331*, 136987. https://doi.org/10.1016/j.energy.2025.136987
18. Liu, Z., Zheng, F., & Li, Y. (2017). Enhancing boiling and condensation co-existing heat transfer in a small closed space by copper foam inserts. *International Journal of Heat and Mass Transfer, 108*, 961–971. https://doi.org/10.1016/j.ijheatmasstransfer.2016.12.088
19. Mahdianikhotbesara, A., Sehhat, M. H., & Hadad, M. (2022). A numerical and experimental study into thermal behavior of micro friction stir welded joints of Al 1050 and copper sheets. *Applied Mechanics and Materials Research*. https://doi.org/10.4028/p-01ag12
20. Miranda, J. O., Hermens, M., Nikitin, I., Kouznetsova, V. G., Sluis, O., Ras, M. A., Reparaz, J. S., Wagner, M. R., Sledzinska, M., Gomis-Bresco, J., Torres, C. M., & Volz, S. (2016). Measurement and modeling of the effective thermal conductivity of sintered silver pastes. *International Journal of Thermal Sciences, 108*, 185–194. https://doi.org/10.1016/j.ijthermalsci.2016.05.014
21. Padrah, I., Pásztor, J., & Farmos, R. (2019). Design and implementation of laboratory equipment for studying heat transfer by conduction. *Műszaki Tudományos Közlemények, 11*(1), 153–156.
22. Qiu, G., Zhu, S., Wang, K., Wang, W., Hu, J., Hu, Y., Zhi, X., & Qiu, L. (2025). Effect of thermal conduction in cylinder wall on in-cylinder heat transfer in high-pressure liquid hydrogen pumps. *International Journal of Hydrogen Energy, 102*, 937–946. https://doi.org/10.1016/j.ijhydene.2025.01.086
23. Rana, S., & Kumar, A. (2019). FEA-based design and thermal contact conductance analysis of steel and Al rough surfaces. *International Journal of Applied Engineering Research, 13*(16), 12715–12724.

24. Rasaq, B., & Ogundare, R. T. (2018). Determination of thermal conductivities of some metal materials and clay. *Physical Science International Journal*, *19*(3), 1–8. https://doi.org/10.9734/PSIJ/2018/42962
25. Talaghat, M. R., & Jokar, S. M. (2017). Determination of heat transfer parameters using finite integral transform and experimental data. *Heat and Mass Transfer*, *53*, 3529–3544. https://doi.org/10.1007/s00231-017-2067-7
26. Tritt, T. M. (Ed.). (2005). *Thermal conductivity: Theory, properties, and applications*. Springer. https://doi.org/10.1007/b136496
27. Wang, J., Wu, Z., Mao, C., Zhao, Y., Yang, J., & Chen, Y. (2018). Effect of electrical contact resistance on measurement of thermal conductivity for metallic nanowires. *Scientific Reports*, *8*, 23291. https://doi.org/10.1038/s41598-018-23291-9
28. Callister, W. D., & Rethwisch, D. G. (2009). *Materials science and engineering* (9th ed.). Wiley.
29. Xu, F., Li, G., Liao, J., Ji, W., Yi, Z., & Wei, L. (2025). An improved design of water-cooled beam in reheating furnace based on conduction model. *Thermal Science and Engineering Progress*, *61*, 103567. https://doi.org/10.1016/j.tsep.2025.103567
30. Xu, H. J., Xing, Z. B., Wang, F. Q., & Cheng, Z. M. (2019). Review on heat transfer of nanofluids in porous media: Fundamentals and applications. *Chemical Engineering Science*, *195*, 462–483. https://doi.org/10.1016/j.ces.2018.09.045
31. Yang, S., Wang, J., Dai, G., Yang, F., & Huang, J. (2021). Controlling macroscopic heat transfer with thermal metamaterials: Theory, experiment, and application. *Physics Reports*, *908*, 1–65. https://doi.org/10.1016/j.physrep.2020.12.006
32. Zain-ul-Abdein, M., Raza, K., Khalid, F. A., & Mabrouki, T. (2015). Numerical investigation of the effect of interfacial thermal resistance on copper/diamond composites. *Materials & Design*, *86*, 248–258. https://doi.org/10.1016/j.matdes.2015.07.059
33. Zhang, J., Dehkordi, M. H. R., Kholoud, M. J., Azimy, H., & Daneshmand, S. (2025). Experimental and numerical study of melt flow and heat transfer during dissimilar laser welding. *Optics & Laser Technology*, *180*, 111521. https://doi.org/10.1016/j.optlastec.2024.111521
34. Zhao, D., Qian, X., Gu, X., Jajja, S. A., & Yang, R. (2018). Measurement techniques for thermal conductivity and interfacial thermal conductance. *Journal of Heat Transfer*, *140*(10), 100907. https://doi.org/10.1115/1.4034605